TẠP CHÍ KHOA HỌC
TRƯỜNG ĐẠI HỌC QUY NHƠN

Ảnh hưởng của pH đến quá trình hấp phụ - xúc tác quang của WS_2

Nguyễn Thị Thanh Bích[1], Nguyễn Đức Nhân[1], Huỳnh Hữu Điền[1], Nguyễn Tống Yến Như[1], Phạm Thị Yến Nhi[1], Nguyễn Văn Phúc[2], Trương Duy Hướng[2], Võ Viễn[2,*]

[1]Khoa Sư phạm, Trường Đại học Quy Nhơn, Việt Nam
[2]Viện Nghiên cứu ứng dụng Khoa học và công nghệ, Trường Đại học Quy Nhơn, Việt Nam

Ngày nhận bài: 18/03/2020; Ngày nhận đăng: 18/04/2020

TÓM TẮT

Trong nghiên cứu này, vật liệu vonfram đisunfua đã được điều chế bằng cách nung hỗn hợp H_2WO_4 và thiourea với tỷ lệ khối lượng 1:5 trong dòng khí Ar ở 650 ^oC trong 1 giờ và được ký hiệu là WS_2. Sản phẩm được đặc trưng phổ nhiễu xạ tia X, phổ hồng ngoại, phổ tán sắc năng lượng tia X, ảnh kính hiển vi điện tử quét và phổ phản xạ khuếch tán tử ngoại khả kiến. Kết quả cho thấy mẫu tổng hợp được có cấu trúc đặc trưng của WS_2. Khả năng hấp phụ và xúc tác quang của vật liệu WS_2 được đánh giá qua phản ứng phân hủy thuốc nhuộm cation (rhodamine B) ở khoảng pH từ 1,5 đến 8,0, kết quả cho thấy sự giảm nồng độ RhB trên vật liệu WS_2 khi tăng pH dung dịch từ 1,5 đến 8,0 do ảnh hưởng của sự hấp phụ hơn là quá trình phân hủy hóa học. Đặc biệt ở pH = 4, tương tác tĩnh điện giữa bề mặt của vật liệu mang điện tích âm và thuốc nhuộm cation mạnh nhất, dẫn đến hiệu suất hấp phụ và quang xúc tác đạt tối đa tương ứng 66,98% và 20,88% sau 8 giờ thử nghiệm.

Từ khóa: *WS_2, hấp phụ, xúc tác quang, pH, Rhodamine B.*

**Tác giả liên hệ chính.*
Email: vovien@qnu.edu.vn

JOURNAL OF SCIENCE
QUY NHON UNIVERSITY

Effect of pH on adsorption - photocatalysis of tungsten disulfide

Nguyen Thi Thanh Bich [1], Nguyen Duc Nhan[1], Huynh Huu Dien[1], Nguyen Tong Yen Nhu[1], Pham Thi Yen Nhi[1], Nguyen Van Phuc[2], Truong Duy Huong[2], Vo Vien[2,*]

[1]Faculty of Education, Quy Nhon University, Vietnam
[2]Applied research Institute for science and technology, Quy Nhon University, Vietnam

Received: 18/03/2020; Accepted: 18/04/2020

ABSTRACT

In this work, the tungsten disulfide material was prepared by calcining mixture of H_2WO_4 and thiourea with weigh ratio of 1:5 in Ar gas at 650 ^oC for 1h, and denoted as WS_2. The obtained product was characterized by X-ray diffraction (XRD), infrared spectra (IR), energy-dispersive X-ray spectroscopy (EDS), scan electron microscopy (SEM) and UV-Vis diffuse reflectance spectroscopy (UV-Vis). The relevant characterizations indicated that the main composition of sample is tungsten disulfide. The integrated adsorption and photodegradation of the cationic dye (rhodamine B) on WS_2 was evaluated in a pH range of 1.5 - 8.0, which showed that the decline of RhB degradation rate on WS_2 when increasing solution pH from 1.5 to 8 due to adsorption rather than the photodegradation process. Specifically at pH of 4, the strongest electrostatic interaction between the negatively charged surface of the material and cationic dye resulted in a highest adsorption and photocatalytic efficiency up to 66.98% and 20.88%, respectively, after investigating time of 8 hours.

Keywords: *WS_2, adsorption, photocatalysis, pH, Rhodamine B.*

1. INTRODUCTION

Environmental pollution caused by organic toxic pollutants has become a global concern. In order to solve this problem, a variety of advanced oxidation processes have been widely used, and photocatalysis is now attracting a considerable attention for various applications. Beside metal oxide-based photocatalysts such as TiO_2, ZnO, WO_3, Cu_2O, *etc*., the layered-structure materials transition metal dichalcogenides (TMDs) such as MoS_2 and WS_2 having a band gap of 1.8 eV have been become a promising candidate for photocatalyst.[1-4] Layered MoS_2 with different nanostructures like nanowires, nanorods, and nanotubes, the monolayer and multilayer structures have been also synthesized.[5-10] The layered structure of MoS_2 crystals, with hexagonal arrangement of atoms by covalent bonds in a sequence of S–Mo–S through weak Van der Waals interactions could be suitable for solar cells, photonics, optoelectronics, and catalysts applications.[5,6] Similar to MoS_2 in terms of crystal structure and chemical property, WS_2 also has a narrow band gap making this material could work as a photocatalyst to decompose organic molecules under visible light.[1,3,10,12]

**Corresponding author.*
Email: vovien@qnu.edu.vn

Various reports show that a nano-photocatalyst possessing a high specific surface area performs not only an excellent photocatalytic activity but also a strong adsorption capacity to pollutants.[13,14] Furthermore, the adsorption process can strongly affect the photocatalytic efficiency of decomposing pollutants due to the fact that both the adsorption and the photoinduced reactive species mainly occur on the surface of the material.[14,16] Most available photocatalytic studies have ignored or ejected the adsorption kinetics by assuming the adsorption - desorption interaction reaching the equilibrium, then considering the decrease in the concentration of pollutants is due to photocatalytic process.[17,19] However, the adsorption-adsorption equilibrium cannot be achieved in the photocatalytic reaction due to the activation of radicals, which causes the concentration of the adsorbent on the catalyst to decrease continuously when illuminated.[20] Meanwhile, few studies have been published involving the effects of adsorption on photocatalytic degradation to remove pollutants. Recently, Luo et al. showed that adsorption process can promote the decomposition of Red 120 dye on the g-C_3N_4 catalyst with the proposed Elovich kinematic model.[21] This paper focuses on the synergy between adsorption and photocatalysis of a typical catalyst, WS_2. To consider the adsorption capacity, in this study, we changed the pH of the reaction solution and used Rhodamine B (RhB) as a target molecule.

2. EXPERIMENT

2.1. Chemicals

The chemicals used in the synthesis were H_2WO_4, $(NH_2)_2CS$, rhodamine B purchased from Xilong Chemical Co. Ltd. (China) with the purity over 99% and no further modification.

2.2. Preparation of material

The WS_2 material was synthesized via a facile solid-state reaction by the following procedure: a mixture of tungstic acid and thiourea with weigh ratio of 1:5 was added to a solvent of 10 mL of distilled water and 30 mL of C_2H_5OH with stirring at 40 °C. After 5 hours, the solid was collected and then dried for 12 hours at 80°C. The obtained solid was finely ground and transferred to a ceramic cup, covered closely with aluminum foil, and then annealed at 650°C for 2 h under Ar gas. The resulting material was rinsed several times with distilled water and C_2H_5OH, then dried at 80 °C for 12 hours, and denoted as WS_2.

2.3. Material characterization

Powder X-ray diffraction (XRD) patterns of sample were recorded by a D8 Advance Xray diffractometer with Cu Kα radiation (λ = 1.540Å) at 30 kV and 0.01 A. Infrared spectra (IR) of material were measured by IRPrestige-21 (Shimadzu). The SEM image and nergy-dispersive X-ray spectroscopy (EDS) of sample were recorded on Nova Nano SEM 450. UV-Vis diffuse reflectance spectroscopy (UV-Vis-DRS) was carried out on Cary 5000 (Varian, Australia).

2.4. Determination of pH_{PZC}

Point of zero charge (pH_{PZC}) of WS_2 material was determined by titration method of measuring pH of 0.1M NaCl solution at 30 °C. In detail, initial pH values (pHi) of 50 mL of 0.1M NaCl solution were adjusted from 1.0 to 12.0 by addition of HCl or NaOH. To the solutions, 0.03 grams of WS_2 were added and stirred for 24 hours. The suspensions were separated and the pH final values (pH_f) were measured. The point of zero charge was pH_i when $pH_i = pH_f$. The pH value of the solutions is measured on the HANA HI2211 pH meter.

2.5. Photocatalytic activity evaluation

The adsorption and photocatalytic activity of WS_2 was evaluated by the removal efficiency of rhodamine B (RhB) in aqueous solution at the dark and under the light of LED (220V- 30W). The concentration change of RhB was measured on UV-Vis spectrophotometer (CECIL CE2011) at the wavelength of 553 nm.

The efficiency (h) is calculated by the following expression:

$$h = \frac{C_o - C_t}{C_o} 100\ (\%)$$

Where C_o and C_t are the initial concentrations and the concentrations of rhodamine B solution (mg/L) at time t (hour).

3. RESULTS AND DISCUSSION

The crystal structure and phase of WS_2 sample were analyzed by XRD. As seen in Figure 1, the XRD pattern of WS_2 exhibits main peaks at 2θ = 14.3°; 32.8°; 39.5°; 43.9°; 58,4° and 69,1° corresponding to the (002), (101), (103), (006), (110) and (201) planes, respectively. The peaks match well with the reference of WS_2 (JPCDS card No. 002-0131), confirming that the WS_2 has a hexagonal crystalline structure. The intensity of the (002) reflection for WS_2 at 2θ = 14.3 shows the characterization of multi-layered WS_2 and high order of the material. The d-spacing was calculated base on the (002) plane using Vulf-Bragg equation to be $d_{002} = \frac{\lambda}{2\sin\theta}$ = 6.2 Å, which is consistent with the previous published articles. [3,22]

The bonding vibrations in the molecular structure of WS_2 sample were further confirmed by IR spectra and shown in Figure 2. The band at 3445 cm^{-1} is attributed to the OH vibration of adsorbed water, while the observed peaks in the region of 500 cm^{-1} - 690 cm^{-1} are attributed to W-S bond and band at 960 cm^{-1} is due to the S-S bond.[3]

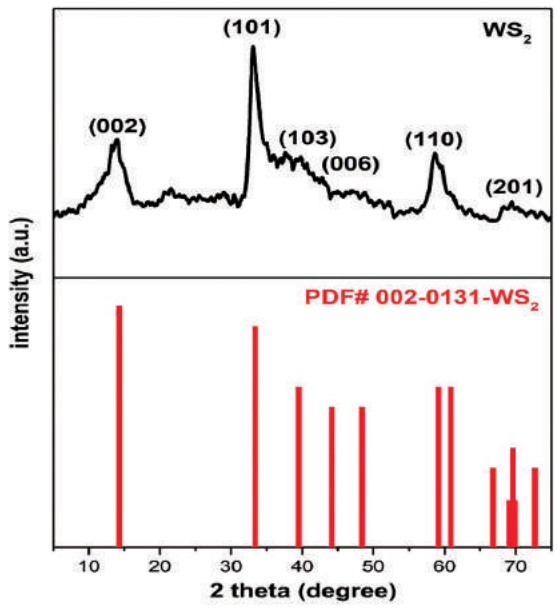

Figure 1. XRD pattern of WS_2.

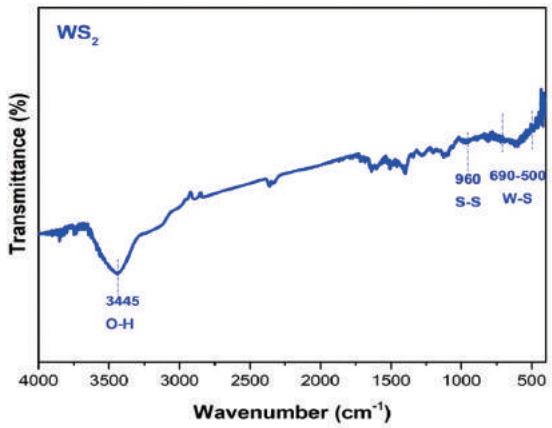

Figure 2. IR spectra of WS_2.

The EDS analysis of WS_2 in Figure 3 shows that W and S are main elements of the material. However, the presence of C and N with insignificant content may come from decomposition of the precursors.

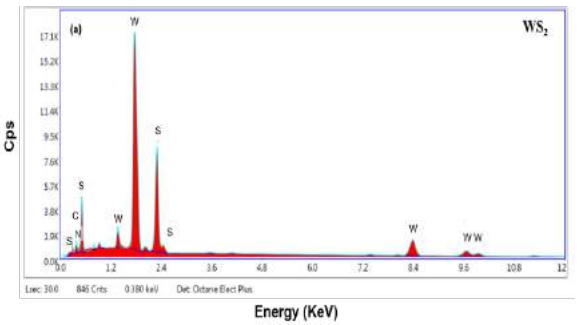

Figure 3. EDS patterns of WS_2.

The morphology of WS_2 was also characterized using SEM. Figure 4 shows that WS_2 is shaped like hydrangea flowers, formed from sheets.

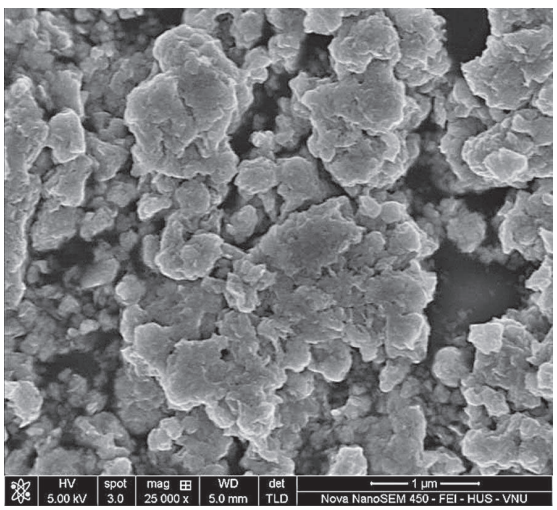

Figure 4. SEM image of WS_2.

The optical properties of WS_2 was characterized by UV-Vis diffuse reflectance spectroscopy and shown in Figure 5.

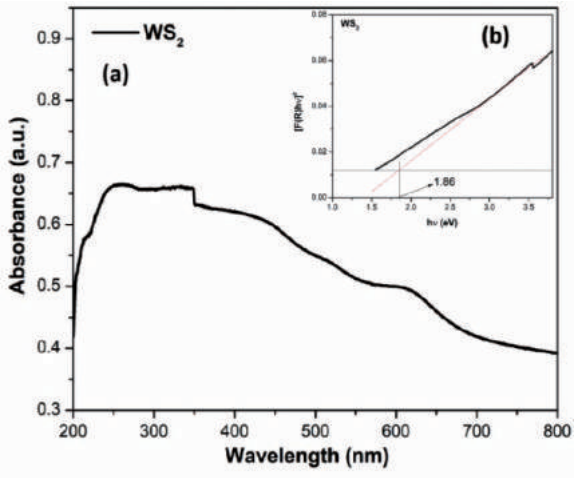

Figure 5. (a) UV-vis spectrum of WS_2 and (b, inset) optical band gap (E_g) of WS_2.

The results show that WS_2 had an absorption band that stretched from the peak in the near ultraviolet region, strong absorption edge and spread to visible light region. The band gap energy of WS_2 is determined via the Kubelka-Munk[23] equation $[F(R)\ h\nu]^2 \sim (\alpha h\nu)^2 \sim (h\nu - E_g)$ with a value of 1.86 eV.[3] This result is consistent with the previous published article.[1,4] With this bandgap energy, WS_2 may exhibit a good photocatalytic performance under visible light.

The effect of the solution pH on the RhB treatment efficiency is mainly due to the change in form of existing RhB molecule and catalyst surface charge in different pH environments. The problem in photocatalysis is distinguishing the adsorption and photocatalytic contribution throughout the total reduction in reactant concentration. The decrease in concentration in dark considered only adsorption (HP), while under light considered including adsorption and catalysis (HP + XT). From there, the difference between these two values ($\Delta\{(HP + XT) - HP\}$) may be considered photocatalyst performance of the material. The conversion of RhB after 8 hours of stirring in dark and after 8 hours under led light is shown in Figures 6, 7, 8 and Table 1.

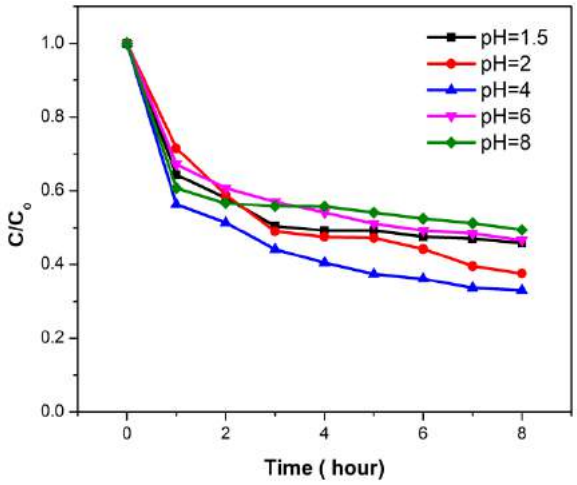

Figure 6. Adsorption efficiency of RhB after 8 hours reaction in dark on WS_2 *(m_{WS_2} = 0.03 g; V_{RhB} = 150mL; C_{RhB} = 30 mg/L).*

The results showed that at pH = 4, the adsorption efficiency of RhB on WS_2 was the highest (HP = 66.98%), with $\Delta\{(HP + XT) - HP\}$ reached 20.88%. The adsorption efficiency decreased in lower pH values (pH = 1.5; 2) or higher pH values (pH = 6, 8), resulting in photocatalytic efficiency at these pH values were also lower than that at pH = 4. This can be explained by electrostatic interactions between the charged surface of WS_2 and the positively charged cationic dye. The pH_{pzc} of WS_2 is shown in Figure 9, estimated to be ~1.5. In aqueous solutions, when $pH < pH_{pzc}$, the surface charge of WS_2 is positive, while it is negative when $pH > pH_{pzc}$. Meanwhile, RhB as a cationic dye dissociate to chloride ions (Cl^-) and cation ammonium in aqueous solution (Figure 10). In the range of the pH above pH_{pzc}, the WS_2 surface carries negative charges, which benefits the adsorption of cationic dyes onto WS_2 through electrostatic interaction. Therefore, the adsorption rates were improved with changing pH values from 1.5 to 4 since the number of negatively charged sites were increased with increasing pH values at this range. At higher pH values, however, specifically at 6 and 8, the - COOH group of RhB began dissociating for negative charges. Therefore, it increases the thrust force on the WS_2 surface, resulting in decreased adsorption capacity when further increasing

pH values.[24] On the other hand, the observed results show that the photodegradation ability of WS_2 declined dramatically with the increase of solution pH from 4 to 8. In a photocatalytic process, •OH is believed to be a strong oxidant for decomposition of organic pollutants and is the main active species at neutral or high pH levels.[25] Moreover, •OH is much easier produced at high pH value, resulting in the enhancement of photocatalytic efficiency.[26,27] As a result, there is a synergistic relationship between adsorption and photocatalysis, in which, adsorption will give good photocatalytic results due to free radicals reacting with organic compounds in the form of adsorption on the catalysts surface rather than they in solution. This result is also observed in the previously published article.[21]

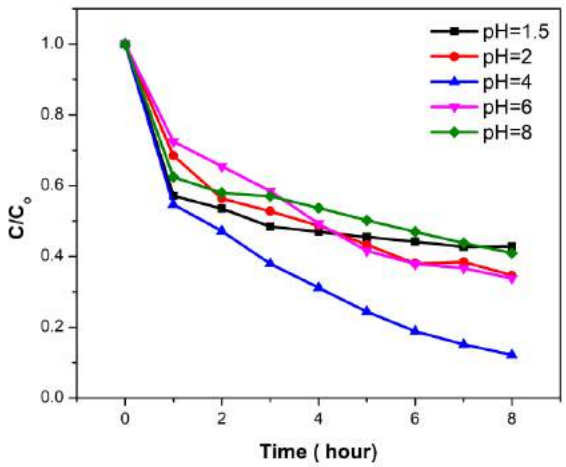

Figure 7. Photocatalytic efficiency of RhB after 8 hours reaction under led light on WS_2 *(m_{WS_2} = 0.03 g; V_{RhB} = 150 mL; C_{RhB} = 30 mg/L, LED light 220V-30W).*

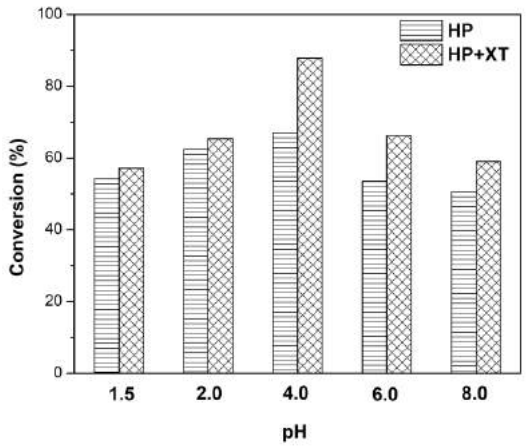

Figure 8. The conversion of RhB after 8 hours reaction in dark and under led light on WS_2.

Table 1. The conversion of RhB after 8 hours reaction in dark and under led light on WS_2.

pH	Conversion of RhB (%)		
	HP	(HP + XT)	Δ (HP+XT) - HP
1.5	54.18	57.11	2.93
2.0	62.40	65.34	2.94
4.0	**66.98**	**87.86**	**20.88**
6.0	53.45	66.24	12.79
8.0	50.59	59.03	8.44

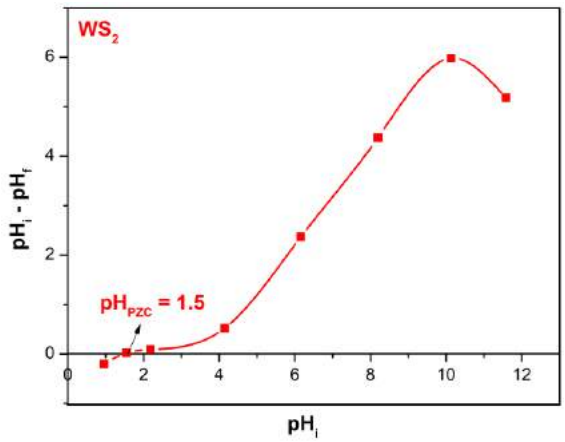

Figure 9. The point of zero charge of WS_2.

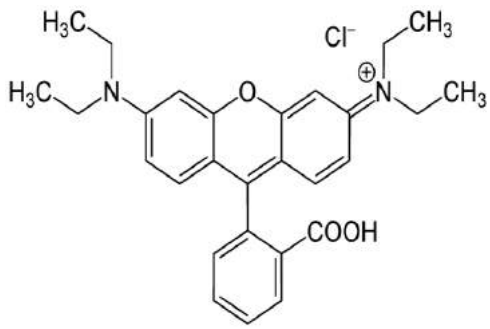

Figure 10. Chemical structure of rhodamine B.

4. CONCLUSIONS

The WS_2 material was synthesized via a facile solid-state calcination of mixture containing H_2WO_4 and thiourea in Ar gas. The synthesized WS_2 material has good adsorption and photodegradation capability towards the cationic dye (rhodamine B) at a wide pH ranges from 1.5 to 8. Especially at pH = 4, the electrostatic interaction between the negatively charged surface of the material and cationic

dye is strongest with a maximum efficiency of 66.98% after in dark for 8 hours and the highest photocatalytic efficiency of 20.88%. There is a synergistic relationship between adsorption and photocatalysis, in which, a high adsorption would give a better photocatalytic results due to free radicals reacting with organic compounds in the form of adsorption on the catalyst surface rather than them in the bulk of solution. Based on the obtained results, WS_2 can be a candidate for organic pollution treatment in the environment. However, further studies should be conducted including modification of the WS_2 material by doping or coupling with other materials in order to change its surface and electrochemical properties.

ACKNOWLEDGEMENT: *This research is conducted within the framework of the student scientific research project for the academic year 2019 - 2020 under the project code S2019.576.13.*

REFERENCES

1. M. S. Akple, J. Low, S. Wageh, A. Ahmed Al-Ghamdi, J. Yu, J. Zhang. Enhanced visible light photocatalytic H_2-production of g-C_3N_4/WS_2 composite heterostructures, *Applied Surface Science*, **2015**, *358*, 196–203.
2. M. Li, L. Zhang, X. Fan, M. Wu, Y. Du, M. Wang, Q. Kong, L. Zhang, J. Shi. Dual synergetic effects in MoS_2/pyridine-modified g-C_3N_4 composite for highly active and stable photocatalytic hydrogen evolution undervisible light, *Applied Catalysis B: Environmental*, **2016**, *190*, 36–43.
3. S. V. P. Vattikuti, C. Byon, V. Chitturi. Selective hydrothermally synthesis of hexagonal WS_2 platelets and their photocatalytic performance under visible light irradiation, *Superlattices and Microstructures*, **2016**, *94*, 39-50.
4. Y. Sang, Z. Zhao, M. Zhao, P. Hao, Y. Leng, H. Liu. From UV to Near-Infrared, WS_2 Nanosheet: A Novel Photocatalyst for Full Solar Light Spectrum Photodegradation, *Adv. Mater.*, **2014**, 1-7.
5. S. G. Alexander, S. B. Ivan, D. L. Natalia, I. B. Mikhail, Y. A. Mikhail. Structural properties and phase transition of exfoliated-restacked molybdenum disulfide, *J. Phys. Chem. C*, **2013**, *117*, 8509-8515.
6. S. V. P. Vattikuti, C. Byon, V. Chitturi. Synthesis of MoS_2 multi-wall nanotubes using wet chemical method with H_2O_2 as growth promoter, *Superlattice. Microst.*, **2015**, *85*, 124–132.
7. S. V. P. Vattikuti, C. Byon, C. V. Reddy, J. Shim, B. Venkatesh. Co-precipitation synthesis and characterization of faceted MoS_2 nanorods with controllable morphologies, *Appl. Phys. A*, **2015**, *119*, 813–823.
8. X. Wang, Z. Zhang, Y. Chen, Y. Qu, Y. Lai, J. Li. Morphology-controlled synthesis of MoS_2 nanostructures with different lithium storage properties, *J. Alloy. Compd.*, **2014**, *600*, 84– 90.
9. Z. Zeng, Z. Yin, X. Huang. Single-layer semiconducting nanosheets: High-yield preparation and device fabrication, *Angewandte Chemie.*, **2011**, *50*, 11093–11097.
10. Y. Wu, Z. Liu, J. Chen, X. Cai, P. Na. Hydrothermal fabrication of hyacinth flower-like WS_2 nanorods and their photocatalytic properties, *Materials Letters*, **2017**, *189*, 282–285.
11. Y. Ma, J. Li, E. Liu, J. Wan, X. Hu, J. Fan. High efficiency for H_2 evolution and NO removal over the Ag nanoparticles bridged g-C_3N_4 and WS_2 heterojunction photocatalysts, *Applied Catalysis B: Environmental*, **2017**, *219*, 467-478.
12. Y. Hou, Y. Zhu, Y. Xu, X. Wang. Photocatalytic hydrogen production over carbon nitride loaded with WS_2 as cocatalyst under visible light, *Applied Catalysis B: Environmental*, **2014**, *156-157*, 122–127.
13. M. I. Zaki, N. E. Fouad, G. A. H. Mekhemer, T. C. Jagadale, S. B. Ogale. TiO_2 nanoparticle size dependence of porosity, adsorption and catalytic activity, *Colloid Surf. A,* **2011**, *385*, 195–200.
14. W. Zou, B. Gao, Y. Ok, L. Dong. Integrated adsorption and photocatalytic degradation of volatile organic compounds (VOCs) using carbon-based nanocomposites: a critical review, *Chemosphere,* **2019**, *218*, 845–859.

15. D. Friedmann, C. Mendive, D. Bahnemann. TiO_2 for water treatment: parameters affecting the kinetics and mechanisms of photocatalysis, *Appl. Catal. B: Environ.,* **2010**, *99*, 398–406.

16. C. B. Mendive, T. Bredow, A. Feldhoff, M. Blesa, D. Bahnemann. Adsorption of oxalate on rutile particles in aqueous solutions: a spectroscopic, electron-microscopic and theoretical study, *Phys. Chem. Chem. Phys.*, **2008**, *10*, 1960–1974.

17. C. Martínez, M. L. Canle, M. I. Fernández, J. A. Santaballa, J. Faria. Kinetics and mechanism of aqueous degradation of carbamazepine by heterogeneous photocatalysis using nanocrystalline TiO_2, ZnO and multi-walled carbon nanotubes–anatase composites, *Appl. Catal. B: Environ.*, **2011**, *102*, 563–571.

18. H. S. Son, S. J. Lee, I. H. Cho, K. D. Zoh. Kinetics and mechanism of TNT degradation in TiO_2 photocatalysis, *Chemosphere*, **2004**, *57*, 309–317.

19. P. Ji, J. Zhang, F. Chen, M. Anpo. Study of adsorption and degradation of acid orange 7 on the surface of CeO_2 under visible light irradiation, *Appl. Catal. B: Environ.*, **2009**, *85*, 148–154.

20. G. Xue, H. Liu, Q. Chen, C. Hills, M. Tyrer, F. Innocent. Synergy between surface adsorption and photocatalysis during degradation of humic acid on TiO_2/activated carbon composites, *J. Hazard. Mater.*, **2011**, *186*, 765–772.

21. Y. Luo, X. Wei, B. Gao, W. Zou, Y. Zheng, Y. Yang, Y. Zhang, Q. Tong, L. Dong. Synergistic adsorption-photocatalysis processes of graphitic carbon nitrate ($g\text{-}C_3N_4$) for contaminant removal: Kinetics, models, and mechanisms. *Chemical Engineering Journal*, **2019**, 122019(1-7).

22. Y. Q. Zhu, T. Sekine, K. S. Brigatti, S. Firth, R. Tenne, R. Rosentsveig, H.W. Kroto, D. R. M. Walton. Shock-Wave Resistance of WS_2 Nanotubes, *Journal of the American Chemical Society*, **2003**, *125*(5), 1329–1333.

23. P. Kubelka, F. Munk. Ein Beitrag zur Optik der Farbanstriche, *Zeits. f. Techn. Physik*, **1931**, *12*, 593–601.

24. P. Qin, Y. Yang, X. Zhang, J. Niu, H. Yang, S. Tian, J. Zhu, M. Lu. Highly efficient, rapid, and simultaneous removal of cationic dyes from aqueous solution using monodispersed mesoporous silica nanoparticles as the adsorbent, *Nanomaterials*, **2017**, *8*(1), 4(1-14).

25. Z. Shourong, H. Qingguo, Z. Jun, W. Bingkun. A study on dye photoremoval in TiO_2 suspension solution, *Journal of Photochemistry and Photobiology A: Chemistry*, **1997**, *108*(2-3), 235–238.

26. C. Galindo, P. Jacques, A. Kalt. Photodegradation of the aminoazobenzene acid orange 52 by three advanced oxidation processes: UV/H_2O_2, UV/TiO_2 and VIS/TiO_2, *Journal of Photochemistry and Photobiology A: Chemistry*, **2000**, *130*(1), 35–47.

27. I. K. Konstantinou, T. A. Albanis. TiO_2-assisted photocatalytic degradation of azo dyes in aqueous solution: kinetic and mechanistic investigations, *Applied Catalysis B: Environmental*, **2004**, *49*(1), 1–14.